Pramāṇa, Vol. 19, No. 4, October 1982, pp. 399–412. © Printed in India.

K-shell ionisation cross-sections of Cu, Ge, Mo, Ag and Sn by protons of energy 0·3 to 1·8 MeV

D BHATTACHARYA and S K MITRA
Tata Institute of Fundamental Research, Bombay 400 005, India

MS received 10 April 1982

Abstract. *K*-shell ionisation cross secions of Cu, Ge, Mo, Ag and Sn in proton impact have been measured systematically in the energy range 0·3 to 1·8 MeV. Thin targets have been used in transmission geometry. Data are compared with the predictions of the PWBA and the PWBA modified to include corrections due to Coulomb retardation of the projectile, increased binding of the target electron during collision and the relativistic nature of the *K*-shell electrons. The intensity ratios K_α/K_β have also been obtained as a function of proton energy for all the five elements.

Keywords. Ionisation; cross-sections; inner-shell; protons; intensity ratios; x-ray.

1. Introduction

In the past few years there has been a considerable revival of interest in the inner-shell ionisation by light charged particles. A large number of investigations have been made for *K* shells leading to a reasonable understanding of the ionisation process. The available experimental data have been summarised in review articles by Rutledge and Watson (1973) and by Gardner and Gray (1978). Until recently, the data have generally been analysed in the light of several models for direct Coulomb ionisation, *e.g.* the plane-wave Born approximation (PWBA) (Merzbacher and Lewis 1958; Madison and Merzbacher 1975), the binary encounter approximation (BEA) (Garcia 1970; Hansen 1973) and the semi-classical approximation (SCA) (Bang and Hansteen 1959). However, the BEA, though formulated on classical grounds, can be obtained from the PWBA by assuming a plane-wave representation of the ejected electron (Taulbjerg 1976) and the SCA and PWBA have been shown to be equivalent for total cross-sections (Taulbjerg 1977). The PWBA has been found to give good agreement with measured cross-sections for incident projectiles of atomic number $\leqslant 4$ and for energies greater than a few MeV (Brandt 1972; Akselsson and Johansson 1974). However, at lower incident energies, the PWBA has been found to over-estimate the cross-sections (Brandt 1972, McDaniel *et al* 1975). Improvements have been proposed to the PWBA by considering certain physical effects not included earlier. The PWBA has been modified by Brandt and his collaborators (Basbas *et al* 1973, 1978; Brandt and Lapicki 1974) to include Coulomb retardation of the incident ion by the target nucleus and increased binding of the target electron due to the presence of the projectile inside the *K*-shell during the collision. Both these modifications, which are important at lower incident velocities, reduce the theoretical cross-sections

and improve the agreement with measurements (McDaniel *et al* 1975; Wilson *et al* 1977).

Relativistic effects which are believed to be important particularly at low incident velocities for heavier targets are expected to increase the theoretical cross sections (Jamnik and Zupančič 1957; Hönl 1933; Hansen 1973; Tricomi *et al* 1977). For heavy targets, the K-shell electrons move with relativistic velocities and so relativistic wave functions should be used in the calculations of the cross-sections. The relativistic K-shell wave-function has a singularity at the origin. This increases the form factor for the large values of momentum transfer which are needed for ionisation by low energy projectiles. The enhancement of the form factor increases the cross-section at low incident velocities and the effect subsides as the velocity increases. Full relativistic calculations are, however, rather involved and the available formulations are not explicit enough to extract numerical values for the individual cross-sections. Recently, Brandt and Lapicki (1979) have prescribed an approximate estimation of the relativistic correction. In this context there is a need to measure absolute K-shell ionisation cross-section for medium-Z elements at low projectile energies and investigate the effect of relativistic and other corrections to the PWBA. These cross-sections are also useful for laboratories involved in analytical studies of trace elements *e.g.* PIXE (Johansson and Johansson 1976).

In this work we have measured the K-shell ionisation cross-sections of Cu, Ge, Mo, Ag and Sn induced by protons in the energy range 0·3 to 1·8 MeV. The intensity ratios K_α/K_β as a function of the projectile energy have also been determined. Similar work using ^{4}He ions as projectiles are being reported elsewhere (Bhattacharya *et al* 1982b). The cross-section data have been compared with the predictions of PWBA with and without modifications for increased binding, Coulomb retardation, and relativistic effects (Basbas *et al* 1973, 1978; Brandt and Lapicki 1974, 1979). The K_α/K_β ratios have been compared with the theoretical predictions of Scofield (1974a, b).

2. Experimental procedure

The experimental procedure is the same as that used in our earlier works (Bhattacharya *et al* 1980, 1982a) and only a brief description will be given here. Protons in the energy range 0·3 to 0·9 MeV were obtained from the 1 MV Cockcroft-Walton generator at this Institute. For the higher energy range the 2 MV van de Graaff accelerator at the Indian Institute of Technology, Kanpur was used. The two sets of measurements were matched at three common energy points, 0·7, 0·8 and 0·9 MeV and were found to be quite consistent with each other. The beam energy calibrations for the accelerators were done by using the 340 keV, 672 keV and 872 keV resonances of the reaction ^{19}F(p, $\alpha\gamma$) ^{16}O and the 1·02 MeV threshold of the reaction $^3T(p, n)$ ^{3}He. After its emergence from the analysing magnet, the proton beam was focussed onto the target through a 1 mm diameter tantalum collimator. Thin targets were used in transmission geometry and the target thicknesses were approximately 100 μg/cm^2 for Cu, Ag and Sn, 90 μg/cm^2 for Ge and 16 μg/cm^2 for Mo. The Cu, Ag and Sn targets were self-supporting; and the Ge and Mo (in oxide form) targets were deposited on carbon backing ($\simeq$ 20 μg/cm^2 thick). After passing through the target the beam was finally collected in a Faraday cup connected to a current integrator. The Fara-

day cup was a 30 cm long narrow tube electrically insulated and placed at the other end of the scattering chamber which had a diameter of 30 cm. This arrangement was made to ensure that secondary electrons do not escape from the Faraday cup. To check this point, an electron suppressor was put between the scattering chamber and the Faraday cup. With a negative voltage of 250 V applied to the electron suppressor there was no noticeable change in the current measured by the current integrator. The electron suppressor was therefore not used in the actual measurements. A cold finger was used in the scattering chamber to avoid any possible carbon build up on the target. Targets were mounted at an angle of 45° with respect to the incident beam and the x-ray detector. To ascertain the target thickness, a silicon surface-barrier detector was placed at 157° to the incident beam to detect back-scattered protons from the target. The surface-barrier detector was covered with an aluminium cap having a 0·4 mm diameter hole at the centre. The area of the hole was carefully measured under a microscope. The solid angle subtended by this detector at the target was $4{\cdot}5 \times 10^{-5}$ sr. Target thicknesses were determined by assuming the scattering at 157° to be purely Rutherford in origin. At low energies, particularly for heavy targets, there are deviations from Rutherford law (L'ecuyer *et al* 1979). However, for the heaviest target used by us, *e.g.* Sn, this deviation is less than a few per cent. Possible target deterioration was checked by taking a few scattered proton spectra with the surface barrier detector before and after each x-ray run. At lower energies ($E_p < 0{\cdot}6$ MeV) the surface barrier detector spectra did not clearly resolve the elastic peaks due to scattering from the target and its backing material. Accordingly, surface-barrier detector spectra taken at higher energies were used to obtain the target thickness and x-ray yields were normalised to the integrated proton current.

Characteristic x-rays from the target were detected by a Si(Li) detector 1 cm diameter by 4·5 mm thick along with a cooled FET preamplifier. This had a resolution (FWHM) of 500 eV at 6·4 keV. The absorbers in the path of the x-rays were two 0·0254 cm thick Be windows, one on the scattering chamber and the other on the detector and a 2 mg/cm^2 thick aluminium foil in front of the detector to cut-off the copious L x-rays. The efficiency of the detector in the same geometry as that used in the actual measurements was determined by using calibrated sources of ^{57}Co, ^{109}Cd and ^{241}Am following the procedure given by Gehrke and Lokken (1971).

The x-ray and surface-barrier detector pulses were recorded in a 400-channel analyser. To avoid any pile-up, the proton current was kept between 50 and 300 nA. Figure 1 shows a typical K x-ray spectrum from an Ag target. The K_α and K_β lines are clearly separated. A background run was taken using a blank aluminium target. No peaks were observed in the region of interest indicating the absence of any contamination lines.

The main sources of error in such measurements are (i) target thickness determination, (ii) proton current measurement, (iii) efficiency determination of the x-ray detector and (iv) counting statistics. The individual contributions in the present measurement due to the above sources were estimated to be about 10%, 5%, 10% and 1 to 3% respectively. Final errors were obtained by adding the above values in quadrature and found to be about 15%. For the intensity ratios, however, the first three sources do not contribute and hence the errors in the ratios are about 5% only.

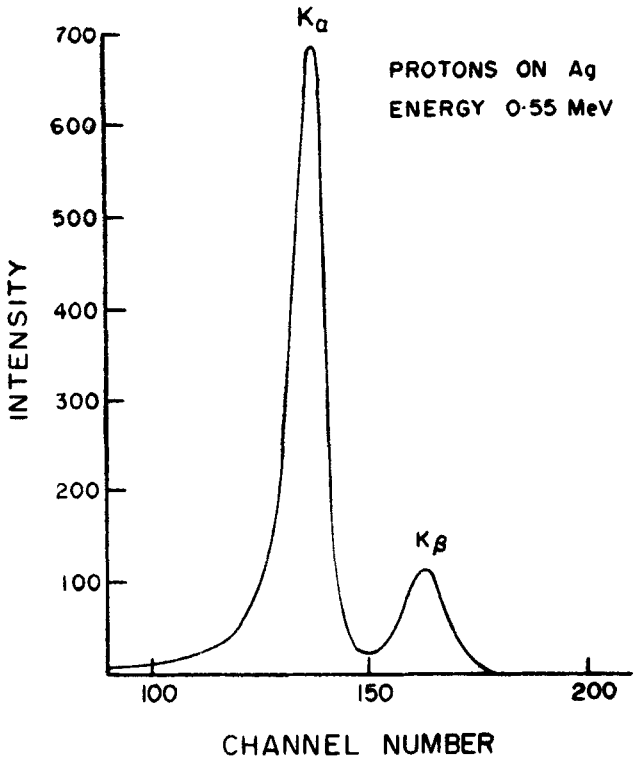

Figure 1. Typical K x-ray spectrum of Ag in 0·55 MeV proton impact.

3. Data analysis

Assuming the x-ray production to be isotropic (Lewis *et al* 1972) the K-shell ionisation cross-sections can be obtained from the following relations

$$\sigma_K^x = (A_\alpha/\epsilon_\alpha + A_\beta/\epsilon_\beta)/N_t\, N_c, \tag{1}$$

$$\sigma_K^i = \sigma_K^x/\omega_K. \tag{2}$$

Here, A_α (A_β) is the observed yield of K_α (K_β) line, N_t is the number of target atoms/cm^2, N_c is the proton current, $\epsilon_\alpha(\epsilon_\beta)$ is the absolute efficiency of the x-ray detector for the K_α (K_β) line and ω_K is the fluorescence yield for the K-shell. The values of ω_K were taken from the recent compilation of Krause (1979). N_t was obtained separately from the surface barrier detector spectra using the expression

$$N_t = N_p/[(\mathrm{d}\,\sigma/\mathrm{d}\,\Omega)_R\, \Omega\, N_c], \tag{3}$$

where N_p is the number of protons detected by the surface-barrier detector, N_c is the beam current measured at the Faraday cup, Ω is the solid angle subtended by the surface-barrier detector at the target and $(d\sigma/d\Omega)_R$ is the Rutherford scattering cross-section at the incident proton energy and the particular scattering angle (157° for the present measurement).

4. Results and Discussions

4.1 *K-shell ionisation cross sections*

The measured K-shell ionisation cross-sections σ_K^i for Cu, Ge, Mo, Ag and Sn are given in tables 1 and 2. In order to compare our data with those of other authors, the data are also plotted in figures 2–6. The predictions of the PWBA (Khandelwal *et al* 1969), the PWBA with corrections due to increased binding and Coulomb retardation (PWBAB, Basbas *et al* 1973, 1978) and PWBAB with the relativistic correction (PWBABR, Brandt and Lapicki 1979) are also shown in the figures. We first note that the predictions of PWBA are two to three times higher than the measured values. Inclusion of "binding" and "Coulomb retardation" corrections (PWBAB) brings the theoretical estimates lower than the data points by about 50%. The predictions of the PWBABR, however, give reasonable agreement (within 20%) for all the elements. In order to bring out the comparison of our data with the predictions of PWBABR more clearly, we have plotted in figure 7 the ratio $\sigma^{\text{expt}}/\sigma^{\text{PWBABR}}$ for all the elements as a function of the scaled velocity parameter ξ_K (ξ_K is the ratio of the projectile velocity to the reduced velocity of the K-shell electron). We find that the ratio has the value $1{\cdot}0 \pm 0{\cdot}2$ which implies that the PWBABR represents the data within 20%. This is quite satisfactory as the experimental uncertainty itself is 15%.

Table 1. Experimental K-shell ionisation cross-sections (in barns) for proton impact on Cu, Ge and Mo (errors in the individual cross-sections are ± 15%; numbers within brackets are exponents of the multiplicative powers of 10).

Cu		Ge		Mo	
E_p (MeV)	σ_i	E_p (MeV)	σ_i	E_p (MeV)	σ_i
0·28	2·1 (−1)	0·33	1·5 (−1)	0·39	5·4 (−3)
0·33	4·0 (−1)	0·37	2·2 (−1)	0·43	8·9 (−3)
0·37	5·7 (−1)	0·42	3·1 (−1)	0·48	1·5 (−2)
0·42	8·3 (−1)	0·46	4·0 (−1)	0·55	2·5 (−2)
0·5	1·5	0·52	6·3 (−1)	0·6	3·8 (−2)
0·56	2·0	0·56	8·0 (−1)	0·66	4·9 (−2)
0·61	2·5	0·6	9·9 (−1)	0·71	6·5 (−2)
0·65	3·0	0·65	1·2	0·77	9·0 (−2)
0·69	3·7	0·71	1·7	0·80	1·3 (−1)
0·74	4·4	0·75	2·1	0·85	1·5 (−1)
0·79	5·4	0·79	2·5	0·9	1·8 (−1)
0·83	6·3	0·91	3·5	1·01	2·9 (−1)
0·87	7·4	1·01	5·2	1·11	4·0 (−1)
0·91	10	1·11	6·4	1·21	5·6 (−1)
1·01	13	1·21	8·7	1·31	7·0 (−1)
1·11	18	1·31	10	1·41	8·9 (−1)
1·21	22	1·41	14	1·51	1·0
1·31	29	1·51	16	1·61	1·4
1·41	37	1·61	20	1·71	1·6
1·51	44	1·71	23	1·81	2·0
1·61	50	1·81	26		
1·71	54				
1·81	69				

Table 2. Experimental *K*-shell ionisation cross-sections (in barns) for proton impact on Ag and Sn (errors in the individual cross-sections are ± 15%; numbers within brackets are exponents of the multiplicative powers of 10).

Ag		Sn	
E_p (MeV)	σ_i	E_p (MeV)	σ_i
0·42	1·9 (−3)	0·42	1·0 (−3)
0·46	3·4 (−3)	0·51	2·1 (−3)
0·51	5·2 (−3)	0·6	3·6 (−3)
0·55	7·8 (−3)	0·7	6·6 (−3)
0·6	1·1 (−2)	0·75	9·0 (−3)
0·64	1·5 (−2)	0·79	1·2 (−2)
0·69	2·1 (−2)	0·83	1·7 (−2)
0·74	2·7 (−2)	0·88	2·4 (−2)
0·82	3·9 (−2)	1·01	3·9 (−2)
0·88	5·3 (−2)	1·11	5·6 (−2)
1·01	9·2 (−2)	1·21	7·9 (−2)
1·11	1·4 (−1)	1·31	1·1 (−1)
1·21	1·8 (−1)	1·41	1·5 (−1)
1·31	2·3 (−1)	1·51	1·9 (−1)
1·41	3·1 (−1)	1·61	2·2 (−1)
1·51	3·9 (−1)	1·71	2·4 (−1)
1·61	4·8 (−1)	1·81	3·1 (−1)
1·71	5·6 (−1)		
1·81	7·1 (−1)		

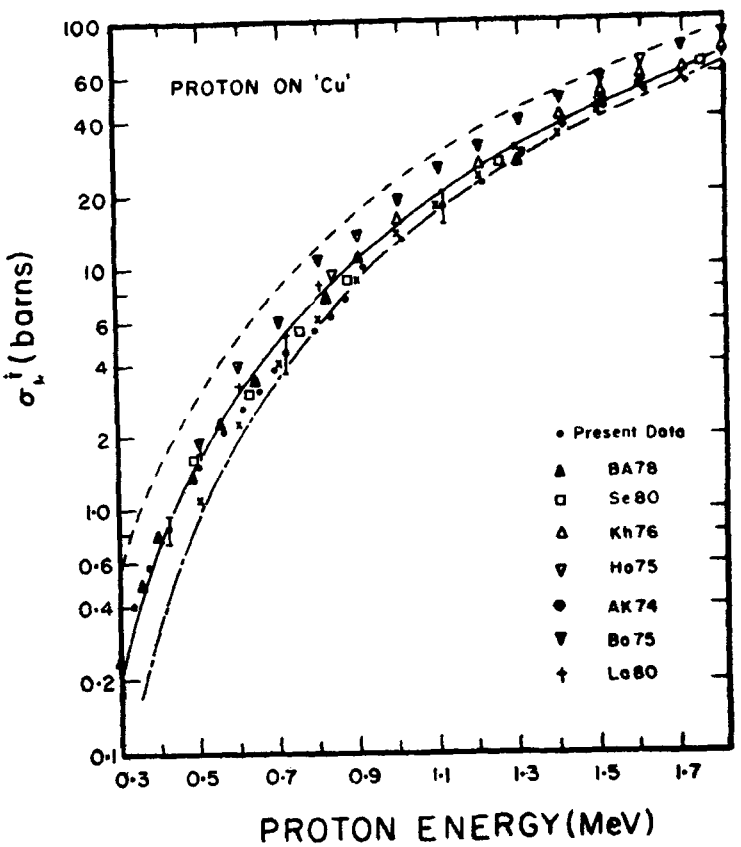

Figure 2. Measured *K*-shell ionisation cross-sections of Cu in proton impact.

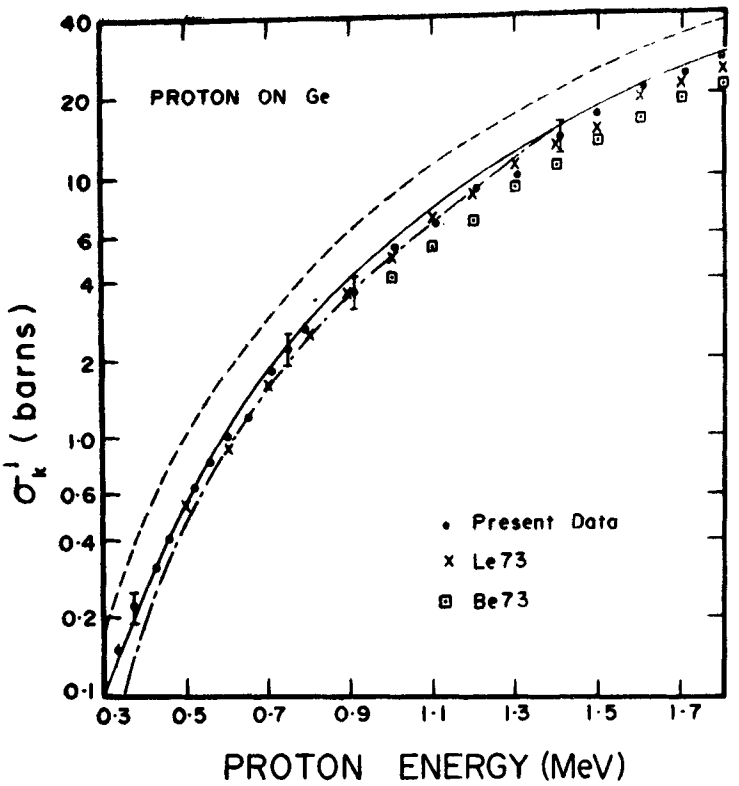

Figure 3. Measured *K*-shell ionisation cross-sections of Ge in proton impact.

4.2 *The intensity ratio K_α/K_β*

Figure 8 shows the variation of the ratio I_{K_α}/I_{K_β} ($= R_{\alpha\beta}$) for all the five elements studied here as a function of the proton energy. The dotted line represents the theoretical values calculated by Scofield (1974a, b). These calculations are based on the assumption that there is a single vacancy in the *K*-shell. In figure 8, we notice that the ratio $R_{\alpha\beta}$ does not show any energy dependence and the measured values agree, within their errors, with the calculated values of Scofield. This indicates that there is very little multiple ionisation in the case of 0·3 to 1·8 MeV proton impact of targets studied here *e.g.* $29 \leqslant Z_2 \leqslant 50$. Similar conclusions were drawn by Wilson *et al* (1977) in their investigation of the *K*-shell ionisation of elements from Nb to Gd.

4.3 *Universal curve for K-shell ionisation*

One feature of inner-shell ionisation cross-sections is their scaling behaviour. Commonly, the quantity $U^2\,\sigma^i/Z_1^2$ plotted as a function of $E/\lambda U$ lies on a single universal curve (Brandt 1972; Madison and Merzbacher 1975). Here U is the binding energy of the particular shell, σ^i is the ionisation cross section by impact of an ion of energy E and charge Z_1 and λ is the mass of the impinging ion in units of electron mass. Figure 9 shows the universal curve obtained from our data and those of others wherever available. Figure 9 also includes our data for Cu, Ge, Mo and Ag in ^{4}He ion impact.

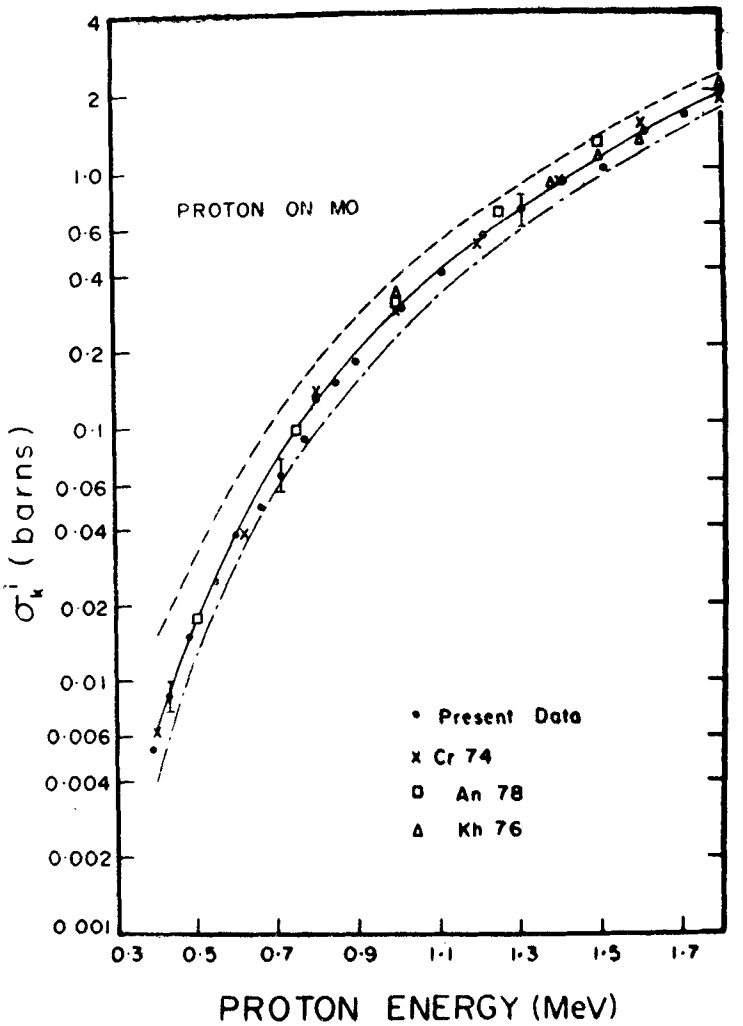

Figure 4. Measured *K*-shell ionisation cross-sections of Mo in proton impact.

We notice that the data for the five elements studied here do lie on a single smooth curve.

4.4 *Empirical formula for K-shell ionisation cross-sections*

In analytical applications it often becomes necessary to estimate in a simple and accurate way *K*-shell ionisation cross-sections for elements for which no data exists. Recently, a simple empirical formula has been proposed by Lopes *et al* (1978). They find that at any given incident proton energy log σ_K^i varies linearly with the atomic number of the target. They have verified this for a small range of Z_2 *e.g.* $20 \leqslant Z_2 \leqslant 26$. In figure 10 is shown a plot of log σ_K^i against Z_2 from our data. We notice that the dependence of log σ_K^i on Z_2 is indeed linear for even a wider range of Z_2 *e.g.* $29 \leqslant Z_2 \leqslant 50$.

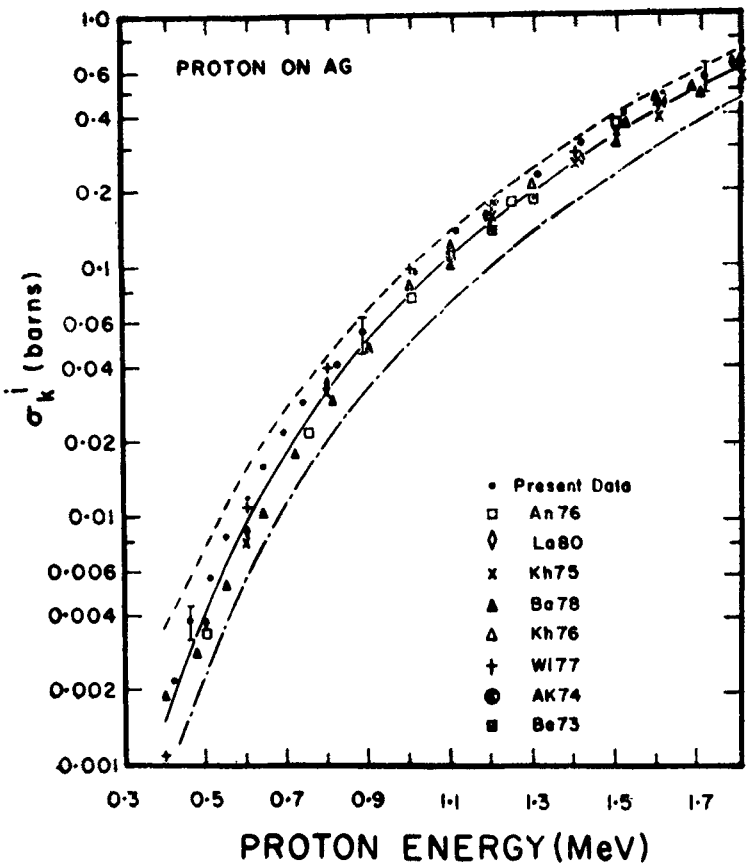

Figure 5. Measured *K*-shell ionisation cross-sections of Ag in proton impact.

4.5 *Comparison with other measurements*

In figures 2–6 we have always included data of other authors wherever available. Most of these have been taken from the compilation of Gardner and Gray (1978) and of Rutledge and Watson (1973). We observe that agreement within two standard deviations exists amongst the data from different laboratories, including ours.

5. Summary and conclusion

K shell ionisation cross sections of Cu, Ge, Mo, Ag and Sn have been measured in proton impact ($0{\cdot}3 \leqslant E_p$ (MeV) $\leqslant 1{\cdot}8$). The PWBA, modified to include corrections due to increased binding, Coulomb retardation and effects due to the relativistic nature of the *K*-shell electrons represents the data quite well for all the elements studied. The intensity ratios K_α/K_β measured by us for the various elements do not show any energy dependence. The values of the ratio K_α/K_β agree, within their errors, with the single-hole calculations of Scofield (1974a, b). This possibly indicates that multiple ionisation does not play any significant role for 0·3 to 1·8 MeV proton impact of elements in the range $29 \leqslant Z_2 \leqslant 50$.

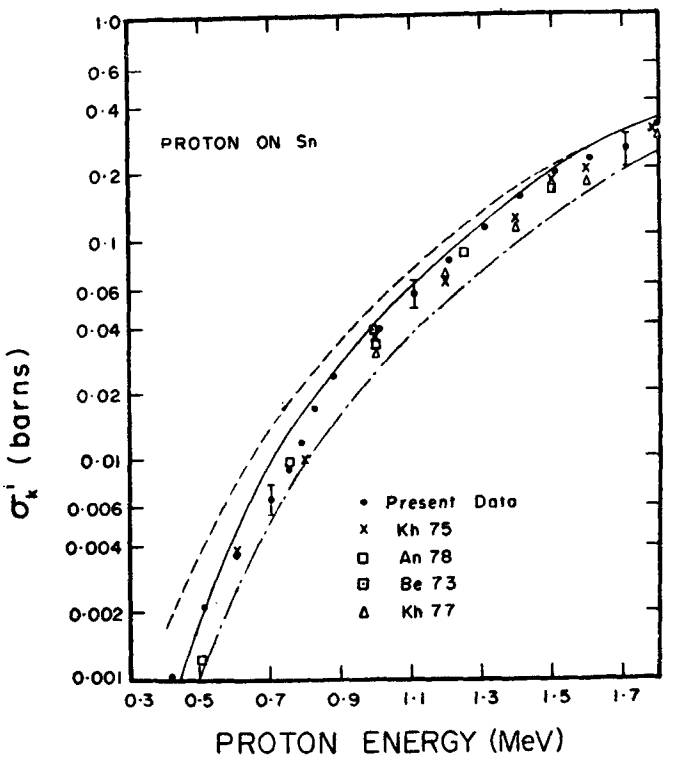

Figure 6. Measured K-shell ionisation cross-sections of Sn in proton impact.

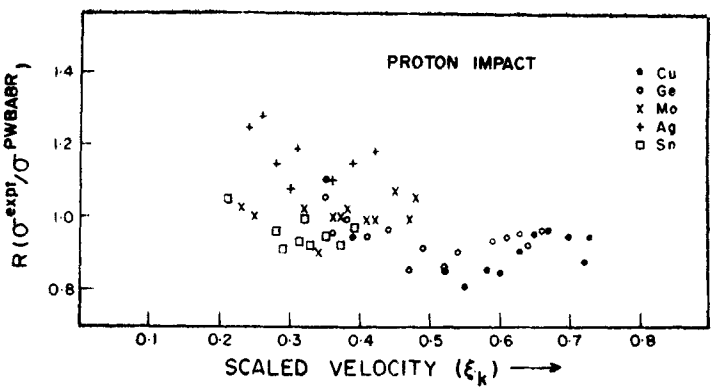

Figure 7. The ratio $\sigma^{expt}/\sigma^{PWBABR}$ in proton impact as a function of the scaled velocity parameter ξ_K.

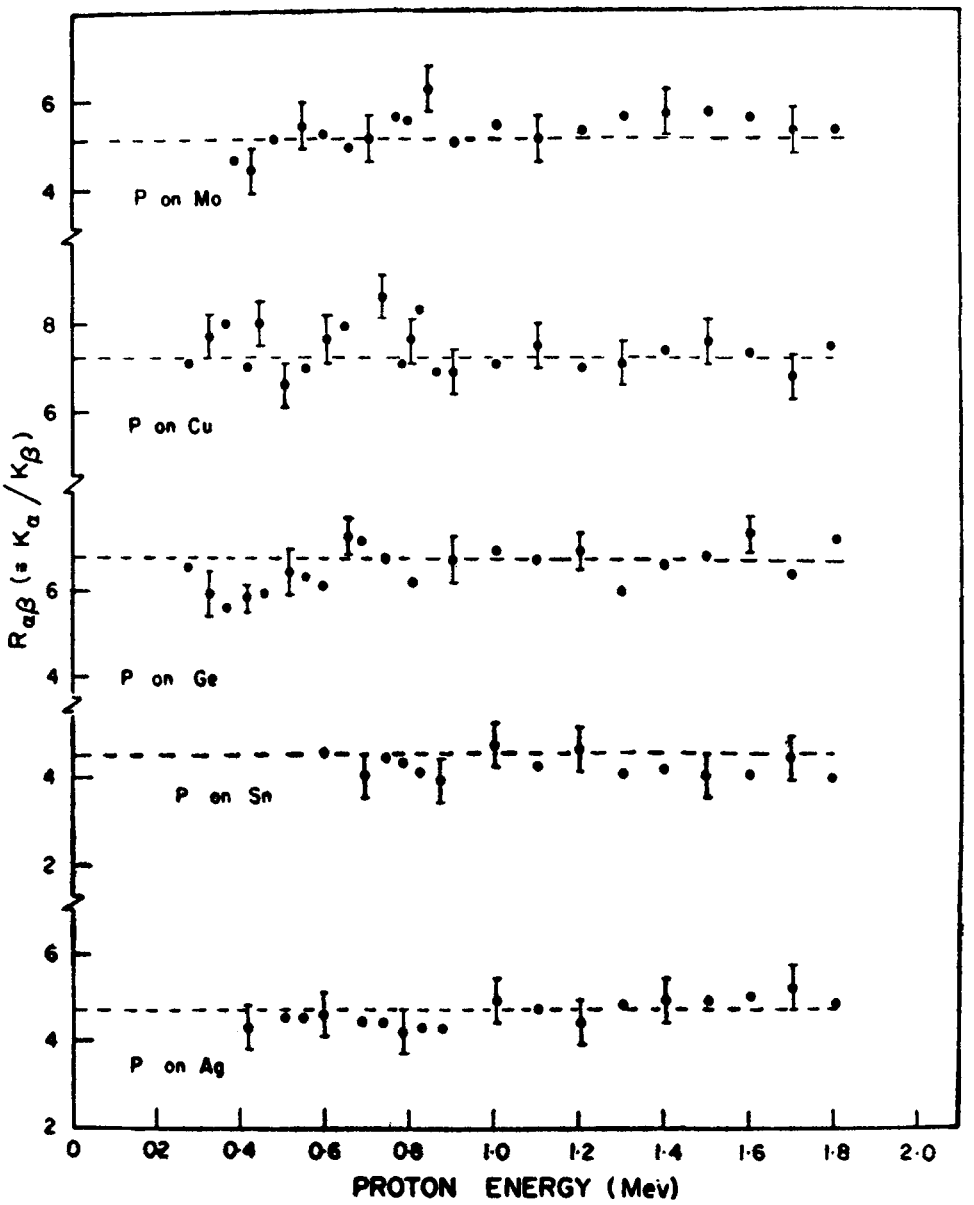

Figure 8. The intensity ratios $R_\alpha\beta = K_\alpha/K\beta$ for Cu, Ge, Mo, Ag and Sn in proton impact. The broken line represents the calculations of Scofield.

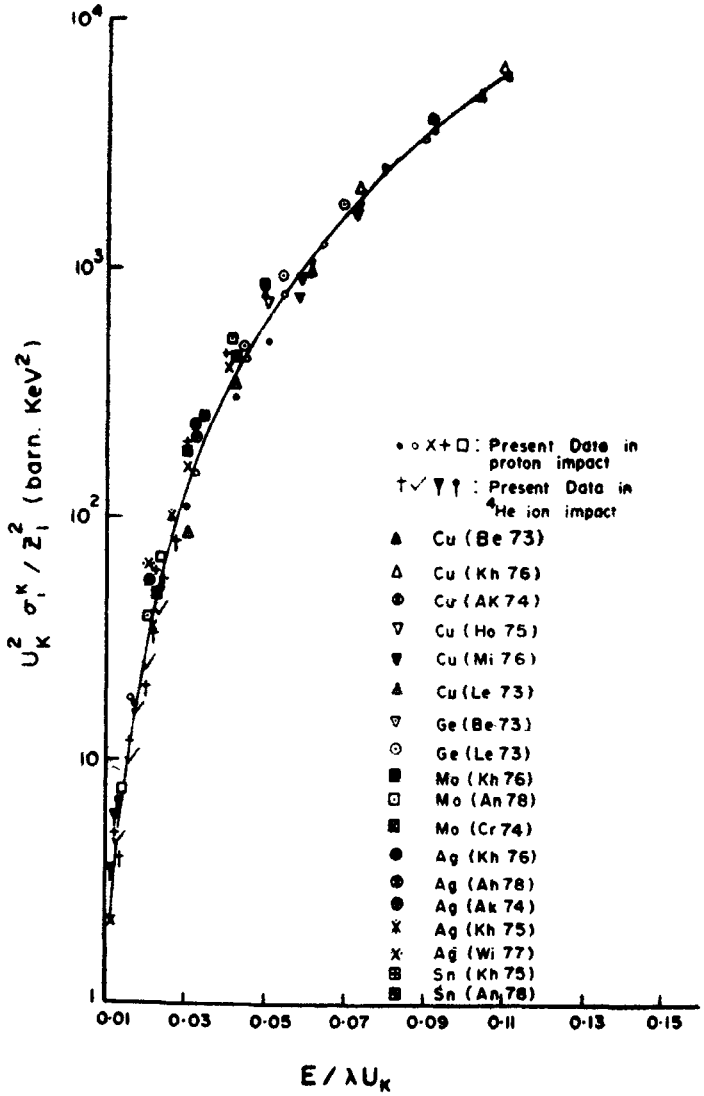

Figure 9. Universal curve for *K*-shell ionisation cross-sections. The full line represents the predictions of the PWBABR.

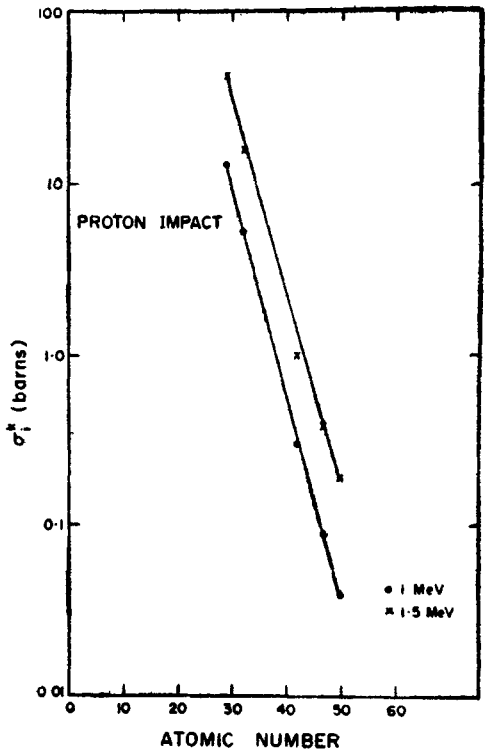

Figure 10. Dependence of the *K*-shell ionisation cross-sections in proton impact on the target atomic number.

Acknowledgements

It is a pleasure to thank Prof. S K Bhattacherjee for his constant encouragement during the course of the experiment and many helpful discussions. The authors are grateful to Prof G K Mehta and Dr S Sen of IIT, Kanpur and the van de Graaff staff for, their helpful cooperation. Thanks are due to members of our detector laboratory for fabricating the Si(Li) detector and the surface barrier detector and also to the Cockcroft-Walton crew for their efficient operation of the accelerator.

References

Akselsson R and Johansson T B 1974 *Z. Phys.* **266** 245
Anholt R 1978 *Phys. Rev.* **A17** 976
Ahholt R, Nagamiya S, Rasmussen J O, Bowman H, Ioannou-Yannou J G and Rauscher E 1976 *Phys. Rev.* **A14** 2103
Bang J and Hansteen J M 1959 *Kgl. Dan. Vidensk. Selsk. Mat. Fys. Medd.* **31** No. 13
Basbas G, Brandt W and Laubert R 1973 *Phys. Rev.* **A7** 983
Basbas G, Brandt W and Laubert R 1978 *Phys. Rev.* **A17** 1655
Bauer C, Mann R and Rudolph W 1978 *Z. Phys.* **A287** 27
Bearse R C, Close D A, Malanify J J and Umbarger C J 1973 *Phys. Rev.* **A7** 1269
Bhattacharya D, Bhattacherjee S K and Mitra S K 1980 *J. Phys.* **B13** 967
Bhattacharya D, Roy A, Bhattacherjee S K and Mitra S K 1982a *J. Phys.* **B 15** 769
Bhattacharya D, Roy A, Bhattacherjee S K and Mitra S K 1982b *J. Phys.* **B** (in press)

Bodart F, Deconnick G and Willk S 1975 *X-ray Spectrometry* **4** 161
Brandt W 1972 *Proc. Int. Conf. Inner-Shell Ionization Phenomena and Future Applications*, Atlanta, Georgia (eds.) R W Fink, S T Manson, J M Palms and P V Rao, p. 948
Brandt W and Lapicki G 1974 *Phys. Rev.* **A10** 474
Brandt W and Lapicki G 1979 *Phys. Rev.* **A20** 465
Criswell T L and Gray T J 1974 *Phys. Rev.* **A10** 1145
Garcia J D 1970 *Phys. Rev.* **A1** 280, 1402
Gardner R K and Gray T J 1978 *At. Data. Nucl. Data. Tables* **21** 515
Gehrke R J and Lokken R A 1971 *Nucl. Inst. Meth.* **97** 219
Hansen J G 1973 *Phys. Rev.* **A8** 822
Hönl H 1933 *Z. Phys.* **84** 1
Hopkins F, Rudiger B, Whittemore A R, Cue N and Dutkiwicz V 1975 *Phys. Rev.* **A11** 1482
Jamnik D and Zupančič C 1957 *Kgl. Dan. Vidensk. Selsk. Mat. Fys. Medd.* **31** No. 2
Johansson S A E and Johansson T B 1976 *Nucl. Instr. Meth.* **137** 473
Khan Md R, Crumpton D and Francois P E 1976 *J. Phys.* **B9** 455
Khan Md R, Hopkins A G, Crumpton D and Francois P E 1977 *X-ray Spectrometry* **6** 140
Khandelwal G S, Choi B H and Merzbacher E 1969 *At. Data* **1** 103
Khelil N A and Gray T J 1975 *Phys. Rev.* **A11** 893
Krause M O 1979 *J. Phys. Chem. Ref. Data* **8** 307
Laegsgaard E, Andersen J U and Hogedal F 1980 *Nucl. Instr. Meth.* **169** 293
Lear R and Gray T J 1973 *Phys. Rev.* **A8** 2469
L'ecuyer J, Davies J A and Matsunami N 1979 *Nucl. Instr. Meth.* **160** 337
Lewis C W, Watson R L and Natowitz J B 1972 *Phys. Rev.* **A5** 1773
Lopes J S, Jesus A P, Fereira G P and Gil F B 1978 *J. Phys.* **B11** 2181
Madison D H and Merzbacher E 1975 *Atomic inner-shell processes* (ed.) B Crasemann **1** 1 (New York: Academic Press)
McDaniel F D, Gray T J and Gardner R K 1975 *Phys. Rev.* **A11** 1607
Merzbacher E and Lewis H W 1958 *Handbuch der Physik* (ed.) S Flügge **34** 166 (Berlin: Springer-Verlag)
Milazzo M and Riccobono G 1976 *Phys. Rev.* **A13** 578
Rutledge C H and Watson R L 1973 *At. Data Nucl. Data Tables* **12** 195
Scofield J H 1974a *Phys. Rev.* **A9** 1041
Scofield J H 1974b *At. Data. Nucl. Data Tables* **14** 121
Sera K, Ishii K, Kamiya M, Kuwako A and Morita S 1980 *Phys. Rev.* **A21** 1412
Taulbjerg K 1976 *Proc. 2nd Int. Conf. on Inner-shell Ionization, Freiburg*, (eds.) W Mehlhorn and R Brenn (Freiburg: Universität Freiburg) p. 130
Taulbjerg K 1977 *J. Phys.* **B10** L 341
Tricomi J, Duggan J L, McDaniel F D, Miller P D, Chaturvedi R P, Wheeler R M, Lin J, Kuenhold K A, Rayburn L A and Cipolla S J 1977 *Phys. Rev.* **A15** 2269
Wilson S R, McDaniel F D, Rowe J R and Duggan J L 1977 *Phys. Rev.* **A16** 903